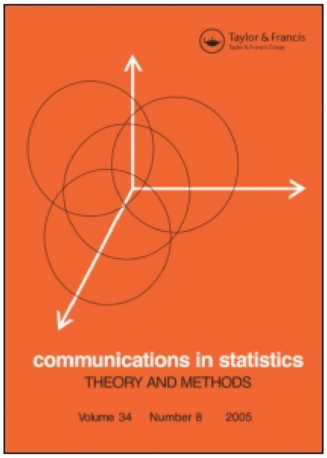

Communications in Statistics - Theory and Methods
Publication details, including instructions for authors and subscription information:
http://www.informaworld.com/smpp/title~content=t713597238

Euler(p, q) Processes and Their Application to Non Stationary Time Series with Time Varying Frequencies

Eun-Ha Choi [a]; Wayne A. Woodward [b]; Henry L. Gray [b]
[a] Rainbow Technology, Inc.. Washington, DC. USA
[b] The Department of Statistical Science, Southern Methodist University. Dallas, Texas. USA

To cite this Article: Eun-Ha Choi, Wayne A. Woodward and Henry L. Gray , 'Euler(p, q) Processes and Their Application to Non Stationary Time Series with Time Varying Frequencies', Communications in Statistics - Theory and Methods, 35:12, 2245 - 2262
xxxx:journal To link to this article: DOI: 10.1080/03610920600853167
URL: http://dx.doi.org/10.1080/03610920600853167

Communications in Statistics—Theory and Methods, 35: 2245–2262, 2006

ISSN: 0361-0926 print/1532-415X online
DOI: 10.1080/03610920600853167

Time Series Analysis

Euler(p, q) Processes and Their Application to Non Stationary Time Series with Time Varying Frequencies

EUN-HA CHOI[1], WAYNE A. WOODWARD[2], AND HENRY L. GRAY[2]

[1]Rainbow Technology, Inc., Washington, DC, USA
[2]The Department of Statistical Science, Southern Methodist University, Dallas, Texas, USA

We introduce Euler(p, q) processes as an extension of the Euler(p) processes for purposes of obtaining more parsimonious models for non stationary processes whose periodic behavior changes approximately linearly in time. The discrete Euler(p, q) models are a class of multiplicative stationary (M-stationary) processes and basic properties are derived. The relationship between continuous and discrete mixed Euler processes is shown. Fundamental to the theory and application of Euler(p, q) processes is a dual relationship between discrete Euler(p, q) processes and ARMA processes, which is established. The usefulness of Euler(p, q) processes is examined by comparing spectral estimation with that obtained by existing methods using both simulated and real data.

Keywords Continuous and discrete Euler(p, q) processes; Non stationary; M-stationary; Origin offset; Time deformation.

Mathematics Subject Classification Primary 62M10; Secondary 62M15.

1. Introduction

A variety of natural signals such as "chirps", Doppler signals, bat echolocations, and seismic signals are non stationary due to frequency behavior that changes over time. Gray and Zhang (1988) introduced continuous multiplicative stationary processes (M-stationary processes) to characterize this type of behavior when frequencies change like $(a + bt)^{-1}$. These processes are non stationary in the sense that the usual autocovariance of the processes, $E[(X(t) - \mu)(X(t + \tau) - \mu)]$ depends on time as well as lag τ. However, the multiplicative covariance, $E[(X(t) - \mu)(X(t\tau) - \mu)]$,

Received April 11, 2005; Accepted March 10, 2006
Address correspondence to Wayne A. Woodward, The Department of Statistical Science, Southern Methodist University, Dallas, TX, USA; E-mail: waynew@mail.smu.edu

of an M-stationary process depends only on τ. That is, a continuous M-stationary process is stationary under the multiplicative composition law. M-stationary processes have the same properties as classical stationary processes after a logarithmic transformation of time. Discrete Euler(p) processes were introduced by Gray et al. (2005). These authors showed the discrete Euler(p) model to be useful for analyzing discrete time series data when frequency behavior changes in time like $(a + bt)^{-1}$.

In this article, continuous and discrete Euler(p, q) processes are defined and their properties are developed. We then consider sampling a continuous Euler(p, q) process at the sample points h^k for $h > 1$ and $k = 0, \pm 1, \pm 2$ to obtain a discrete Euler(p, r) process with $r \leq p - 1$. Euler(p, q) models are compared with autoregressive moving average (ARMA) and Euler(p) models on simulated and actual data.

2. Continuous and Discrete Euler(p, q) Processes

In this section, continuous and discrete Euler(p, q) processes are defined and their relationship is discussed.

2.1. *Continuous Euler(p, q) Processes*

Continuous M-stationary processes, as defined by Gray and Zhang (1988), satisfy the following.

Definition 2.1. $\{X(t)\}$ is defined as a continuous weakly M-stationary process for $t \in (0, \infty)$ iff for any $t \in (0, \infty)$ and $t\tau \in (0, \infty)$

(i) $E[X(t)] = \mu$
(ii) $Var[X(t)] < \infty$
(iii) $E[(X(t) - \mu)(X(t\tau) - \mu)] = R_X(\tau)$,

where $R_X(\tau)$ is referred to as the multiplicative-autocovariance (M-autocovariance) of $X(t)$.

We will refer to a weakly M-stationary process as simply an M-stationary process throughout. Gray and Zhang (1988) showed that M-stationary processes are stationary processes on the log time scale, which leads to a dual relationship between M-stationary and classical stationary processes. Gray and Zhang (1988) also introduced the continuous Euler(p) process. In Definition 2.2 we define the Euler(p, q) process. Throughout, we make use of the derivatives and their properties formally. Such results can be rigorously established. See Priestley (1981) for further discussion.

Definition 2.2. Let $t \in (0, \infty)$. A continuous Euler(p, q) process is defined to be the M-stationary solution of the equation

$$\begin{aligned} &t^p(X^{(p)}(t) - \mu) + \varphi_1 t^{p-1}\big(X^{(p-1)}(t) - \mu\big) + \cdots + \varphi_p(X(t) - \mu) \\ &\quad = t^q\theta_0 a^{(q)}(t) + t^{q-1}\theta_1 a^{(q-1)}(t) + \cdots + \theta_q a(t), \end{aligned} \tag{1}$$

where $E[X(t)] = \mu$, the φ_i's and θ_i's are constants, and $a(t)$ is M-white noise (see Gray and Zhang, 1988).

Continuous Euler(p, q) processes can be considered to be an extension of continuous Euler(p) processes in the same sense that the ARMA processes are an extension of the AR processes. In other words, the continuous Euler(p) process is the special case of the continuous Euler(p, q) process with $q = 0$. The corresponding Euler moving average process, i.e., Euler$(0, q)$ can be obtained by setting $p = 0$.

The following result shows the relationship between an Euler(p, q) process, $X(t)$, and its dual process, $Y(u)$, where $u = \ln t$ and $Y(\ln t) = X(t)$.

Theorem 2.1. *Let $X(t)$ satisfy the Euler(p, q) model in* (1) *and let $Y(u) = X(t)$ and $\varepsilon(u) = a(t)$ for $t = e^u$. Then the dual process of $X(t)$ satisfies*

$$\begin{aligned}&\left(Y^{(p)}(u) - \mu\right) + \varphi_1^*\left(Y^{(p-1)}(u) - \mu\right) + \cdots + \varphi_p^*(Y(u) - \mu)\\&\quad = \theta_0^*\varepsilon^{(q)}(u) + \theta_1^*\varepsilon^{(q-1)}(u) + \cdots + \theta_q^*\varepsilon(u),\end{aligned} \tag{2}$$

where the φ^*'s and θ^*'s are constants determined by the φ_i's and θ_i's in Eq. (1). *That is, the process $Y(u)$ is a continuous ARMA(p, q) process.*

Proof. We first consider a continuous Euler(1, 1) process (with $\mu = 0$)

$$tX'(t) + \varphi_1 X(t) = t\theta_0 a'(t) + \theta_1 a(t). \tag{3}$$

Let $t = e^u$ and $\varepsilon(u) = a(e^u)$. Then

$$tX'(t) = \frac{dX(e^u)}{du} = \frac{dY(u)}{du}$$

and

$$ta'(t) = \frac{da(e^u)}{du} = \frac{d\varepsilon(u)}{du}.$$

So, $X(t)$ in Eq. (3) has the dual process $Y(u)$ satisfying

$$Y'(u) + \varphi_1^* Y(u) = \theta_0^*\varepsilon'(u) + \theta_1^*\varepsilon(u), \tag{4}$$

where $\varphi_1^* = \varphi_1$, $\theta_0^* = \theta_0$, and $\theta_1^* = \theta_1$. In a similar way, we can extend the dual relationship to higher-order processes. □

It should be noted that although in this example, $\varphi_1^* = \varphi_1$, $\theta_0^* = \theta_0$, $\theta_1^* = \theta_1$, etc., this will not be true in general. *Note:* $X(t)$ will be referred to as an M-stationary solution if $X(e^u) = Y(u)$ is stationary, $u \in (-\infty, \infty)$.

2.2. *Discrete Mixed Euler Processes*

Now we consider the more general logarithmic transformation $Y(u) = X(h^u)$ and $\varepsilon(u) = a(h^u)$ for $h > 1$. That is, $t = h^u$ instead of $t = e^u$. Then

$$\frac{dY(u)}{du} = t\ln h X'(t)$$

and

$$\frac{d\varepsilon(u)}{du} = t \ln ha'(t).$$

The φ_i^*'s and θ_i^*'s in the dual model are determined by h as well as the φ_i's and θ_i's.

We next introduce the concept of a discrete M-linear process (see Vijverberg, 2002).

Definition 2.3. Let $h > 1$ and $t \in S$ where $S = \{t : t = h^k, k = 0, \pm 1, \pm 2, \dots\}$. Then $\{X(t)\}$ is called a discrete M-linear process if for all $t = h^k \in S$,

$$X(t) - \mu = \sum_{j=0}^{\infty} \psi_j a_{h^{k-j}}$$

where a_t is white noise.

The discrete Euler(p, q) processes to be discussed here is an extension of the discrete Euler(p) processes discussed by Gray et al. (2005).

Definition 2.4. Let $h > 1$ and let $S = \{t : t = h^k, k = 0, \pm 1, \pm 2, \dots\}$. Then $\{X(t)\}$ is defined as a discrete M-stationary process if for all $t \in S$,

(i) $E[X(t)] = \mu$
(ii) $Var[X(t)] < \infty$
(iii) $E[(X(t) - \mu)(X(t\tau) - \mu)] = R_X(\tau)$.

Clearly, $Var(X(t)) = R_X(h^0) = R_X(1)$ from (iii). Gray et al. (2005) consider the dual process $\{Y_k\}$ defined by $Y_k = X(h^k)$, $k = 0, \pm 1, \dots$ from which it follows that the covariance of the dual process, i.e., $C_Y(k)$, is given by $C_Y(k) = R_X(h^k)$. Consequently, $\{X(t)\}$ is discrete M-stationary if and only if $\{Y_k\}$ is stationary. Gray et al. (2005) also define the discrete M-spectrum, $G_X(f^*)$, as

$$G_X(f^*) = \sum_{k=-\infty}^{\infty} h^{-2\pi i f^* k} R_X(h^k)$$

where $h > 1$, $|f^* \ln h| < 1/2$, and f^* is referred to as the M-frequency, and they point out that $G_X(f^*) = S_Y(f)$ where $|f| = |f^* \ln h|$ and $S_Y(f)$ is the usual spectrum of the dual process.

Definition 2.5. Let $h > 1$ and $t \in S$, where $S = \{t : t = h^k, k = 0, \pm 1, \pm 2, \dots\}$. Then $X(t)$ is a discrete mixed Euler Autoregressive Moving-Average process (Euler(p, q) if

$$\begin{aligned}(X(t) - \mu) - \varphi_1(X(t/h) - \mu) - \cdots - \varphi_p(X(t/h^p) - \mu) \\ = \theta_0 a(t) - \theta_1 a(t/h) - \cdots - \theta_q a(t/h^p)\end{aligned} \tag{5}$$

which can be written as

$$\Phi(B)(X(h^k) - \mu) = \Theta(B)a(h^k),$$

where $a(t)$ is M-white noise, $h > 1$, $\Phi(B)$, and $\Theta(B)$ have no common factors, and where $\phi_p \neq 0$ and $\theta_q \neq 0$.

Clearly the discrete Euler(p, q) models contain the discrete Euler(p) process of Gray et al. (2005) as the special case with $q = 0$. In the following we assume without loss of generality that $\mu = 0$, and describe the dual relationship between the Euler(p, q) and ARMA(p, q) models. This relationship produces several useful properties of the Euler(p, q) process.

Theorem 2.2. *If $\{X(h^k)\}$ satisfies the Euler(p, q) model in* (5), *then its dual process $Y_k = X(h^k)$ is the discrete ARMA(p, q) process $\{Y_k : k = 0, \pm 1, \ldots\}$ given by*

$$Y_k - \varphi_1 Y_{k-1} - \cdots - \varphi_p Y_{k-p} = \theta_0 \varepsilon_k - \theta_1 \varepsilon_{k-1} - \cdots - \theta_q \varepsilon_{k-q}, \tag{6}$$

where ε_k is white noise and, the φ_i's and θ_i's are the same coefficients as in (5).

Proof. Let $X(h^k) = Y_k$ and $a(h^k) = \varepsilon_k$, and the result follows immediately. □

The special case $p = 0$ is a discrete Euler(p, q) process that has an MA(q) dual process. The discrete Euler(p, q) processes can be regarded as the resulting process obtained by observing an underlying continuous Euler(p, q) process at h^k for $h > 1$ and $k = 0, 1, \ldots$. The following theorem interprets the relationship between continuous and discrete Euler(p, q) processes.

Theorem 2.3. *Let $X(t)$ be a continuous Euler(p, q) process for $t \in (0, \infty)$. When the continuous Euler(p, q) ($q < p$) process is sampled at the points $h^{k\Lambda}$ for $h > 1$ and Λ sufficiently small, where $k = 0, 1, \ldots, n$, the resulting process is a realization from a discrete Euler(p, r) process where $r \leq p - 1$.*

Proof. Let $X(t)$ be a continuous Euler(p, q) for $q < p$ satisfying

$$\begin{aligned} &t^p X^{(p)}(t) + \varphi_1 t^{p-1} X^{(p-1)}(t) + \cdots + \varphi_p X(t) \\ &\quad = t^q \theta_0 a^{(q)}(t) + t^{q-1} \theta_1 a^{(q-1)}(t) + \cdots + \theta_q a(t). \end{aligned} \tag{7}$$

Then according to Theorem 2.1, the dual process $Y(u)$ exists as a solution of

$$Y^{(p)}(u) + \varphi_1^* Y^{(p-1)}(u) + \cdots + \varphi_p^* Y(u) = \theta_0^* \varepsilon^{(q)}(u) + \theta_1^* \varepsilon^{(q-1)}(u) + \cdots + \theta_q^* \varepsilon(u),$$

where the φ^* and θ^* are constants determined by φ and θ, and where u is a real-valued constant, $Y(u) = X(h^u)$ and $\varepsilon(u) = a(h^u)$. We sample $X(t)$ at $h^{k\Lambda}$ for $h > 1$ and $k = 1, 2, \ldots, n$ and let $Y(k\Lambda) = X(h^{k\Lambda})$. The resulting continuous ARMA(p, q) process, $Y(u)$, is then observed at a uniform sampling interval, Λ, where we assume that the sampling is sufficiently fast to assure that $\frac{1}{2\Lambda}$ is greater than the highest frequency in the continuous dual data. Phadke and Wu (1974) show that when the continuous ARMA(p, q) (where $q < p$) process $Y(u)$ is observed at a uniform sampling interval, Λ, the resulting discrete process is ARMA(p, r), $r \leq p - 1$ in the sense that the autocovariance function of the resulting discrete process is equal to that of the discrete ARMA(p, r), $r \leq p - 1$ model with parameters determined by the parameters of the continuous ARMA(p, q) process. Thus, the outcome discrete process, $Y_k = Y(k\Lambda)$, is an ARMA(p, r), $r \leq p - 1$ that satisfies

$$\Phi(B)Y_k = \Theta(B)\varepsilon_k, \tag{8}$$

where the order of $\Phi(B)$ is p and the order of $\Theta(B)$ is less than or equal to $p - 1$. Equation (8) becomes

$$\Phi(B)X(h^{k\Lambda}) = \Theta(B)a(h^{k\Lambda}), \tag{9}$$

since $X(h^{k\Lambda}) = Y_k$ and $a(h^{k\Lambda}) = \varepsilon_k$. Thus, sampling the continuous Euler(p, q) (for $q < p$) at $h^{k\Lambda}$ for $h > 1$ and $k = 1, 2, 3, \ldots, n$, produces a discrete Euler(p, r) process where $r \leq p - 1$ provided h^{Λ} is sufficiently close to 1. Since $h^{k\Lambda} = (h^{\Lambda})^k = h_1^k$, in the following we will without loss of generality simply refer to the sampling increment h^k. □

Theorems 2.4–2.6 establish properties of Euler(p, q) processes. The proofs are similar to that of Theorem 2.3, and are based on standard results for stationary ARMA processes.

Theorem 2.4. *Let $\{X(h^k)\}$ be a discrete Euler(p, q) process. A necessary and sufficient condition that $\{X(h^k)\}$ is M-stationary is that the dual process, $Y_k = X(h^k)$, is stationary.*

Clearly, an Euler$(0, q)$ processes, either continuous or discrete, is always M-stationary. We next introduce the concept of M-invertibility.

Definition 2.6. If an Euler(p, q) process, $X(h^k)$, can be expressed as

$$\sum_{j=0}^{\infty} \pi_j (X(h^{k-j}) - \mu) = a(h^k), \tag{10}$$

where convergence in (10) is in the mean square sense, then $X(h^k)$ is said to be M-invertible.

The condition $\sum_{j=0}^{\infty} |\pi_j| < \infty$ assures that $\sum_{j=0}^{\infty} \pi_j X(h^{k-j})$ is mean square convergent and thus that $X(h^k)$ is invertible. As in the stationary case, M-invertibility assures that the present events are related with the past in a sensible manner and produces a unique model for a given set of Euler(p, q) M-autocorrelations. The following result relates the concepts of invertibility and M-invertibility.

Theorem 2.5. *Let $h > 1$ and $k = 0, 1, 2, \ldots$. A process $X(h^k)$ is M-invertible if and only if the dual process Y_k is invertible.*

Thus an Euler(p, q) process is M-invertible if and only if the dual process is invertible.

2.3. *Origin Offset and Estimating the Parameters of the Model Fit to the Dual Data*

Since M-stationary processes are not stationary and the correlation function depends on time, in order to properly model these processes it is necessary to estimate the location of the initial observation. We refer to this as the origin offset or the realization offset. With reference to the Euler time scale described by index set S in Definition 2.4, Gray et al. (2005) denote the origin offset by h^j and thus h^{j+k}, $k = 1, \ldots, K$ are the first K observations in Euler time.

As will usually be the case in practice, the realizations analyzed in Sec. 3 are all obtained at equally spaced time points, $t = 1, \ldots, n$, rather than at the Euler time points. In the examples, we denote the estimated origin offset by $\widehat{\Lambda}$ and thus the sampled values are actually estimated to be at $\widehat{\Lambda} + t$. Implementation details regarding the estimation of the origin offset and sampling rate h are discussed in Gray et al. (2005) and Choi (2003).

After the origin offset has been estimated and the equally spaced dual data set has been obtained, then an ARMA model is fit to the dual data. In our implementation, we have used AIC (Akaike, 1973, 1974) to identify the orders p and q, and we use maximum likelihood methods to estimate the ARMA model parameters.

2.4. *Spectral Estimation for Euler(p, q) Processes*

The M-spectrum for an Euler(p, q) process is given in Theorem 2.6 which follows. See Gray et al. (2005) for discussion of the M-spectrum for Euler(p) models.

Theorem 2.6. *The M-spectrum of a discrete Euler(p, q) process $\{X(t)\}$ is given by*

$$G_X(f^*) = \sigma_a^2 \frac{|\Theta(e^{-2\pi i f^* \ln h})|^2}{|\Phi(e^{-2\pi i f^* \ln h})|^2}, \quad |f^*| \leq \frac{1}{2 \ln h}, \tag{11}$$

where $\Phi(B) = 1 - \varphi_1 B - \varphi_2 B^2 - \cdots - \varphi_p B^p$ *and* $\Theta(B) = 1 - \theta_1 B - \theta_2 B^2 - \cdots - \theta_q B^q$. *The corresponding M-spectral density is*

$$g_X(f^*) = \frac{\sigma_a^2 |\Theta(e^{-2\pi i f^* \ln h})|^2}{\sigma_X^2 |\Phi(e^{-2\pi i f^* \ln h})|^2}, \quad |f^*| \leq \frac{1}{2 \ln h}. \tag{12}$$

Proof. Follows at once from Theorem 2.2. □

The M-spectrum is obtained in practice using the relationship $G_X(f^*) = S_Y(f^* \ln h)$ where S_Y denotes the spectrum of the dual. Thus, the M-spectrum describes the time-varying frequency behavior in the original series in terms of the fixed frequencies present in the dual. If, for example, the M-spectrum has a single sharp peak, then this indicates that the time-varying frequencies in the original data can be interpreted by means of a single frequency in transformed time. While such a representation can provide a useful characterization of the frequency behavior in the original data, the M-frequency, f^*, does not usually have a physical interpretation. For this reason, it is useful to convert the information in the M-spectrum to a format in which frequency has its usual interpretation. Gray et al. (2005) define the instantaneous spectrum which is a conversion of the M-spectrum into a format that describes the spectral content in the series across time. The instantaneous spectrum for an Euler(p, q) process is defined as follows.

Definition 2.7. The instantaneous spectrum of an Euler(p, q) process at $t = h^k$ is defined by $S(f, h^k; h^j) = G_X(f^*)$ where $G_X(f^*)$ is given in (11) and where $f^* = \left[\ln\left(\frac{1+fh^{j+k}}{fh^{j+k}}\right)\right]$ where h^j is the origin offset as defined in Sec. 2.3.

3. Application to Simulated Data

In this section, we consider three examples that illustrate the application of Euler(p, q) models to simulated data sets generated from M-stationary processes. For each data set, the best fitted Euler(p, q), Euler(p), and classical ARMA models will be compared. We first consider a realization from a sinusoid-plus-noise model on a log time scale to examine the usefulness of modeling such data with an Euler(p, q) model.

Example 3.1. Let $X(t)$ be defined by

$$X(t) = A\cos[2\pi f^* \ln(t + \Delta) + v] + n(t), \tag{13}$$

where $n(t) \sim N(0, \sigma^2)$, v is uniform $[0, 2\pi]$, and where $A = 15$, $\Delta = 19$, and $f^* = 3$. Then, $X(t)$ is an M-stationary process with M-frequency f^*. A realization of length 111 from this process and $\sigma^2 = 0.01$ is shown in Fig. 1(a) where the elongating behavior can be seen. For this realization an AR(10) model was found to be the best fitting AR(p) model. Because of the time-varying frequency behavior in the data, this model will clearly be poor. An Euler(9) model with $\widehat{\Delta} = 18$ and $h = 1.0176$ was found to be the best fitting Euler(p) model, and an Euler(2, 3) model with $\widehat{\Delta} = 18$ and $h = 1.01748$ was the optimal Euler(p, q) model. The dual series corresponding to the Euler(2, 3) fit is shown in Fig. 1(b).

Table 1 shows the irreducible first- and second-order factors associated with the ARMA(2, 3) model fit to the dual data in Fig. 1(b). This presentation is similar to that used by Gray et al. (2005). The M-frequency associated with $1 - 1.899B + B^2$ is 2.9084, which is very close to the M-frequency, $f^* = 3$ of the process from which the original data were generated. It should also be noted that the M-frequency

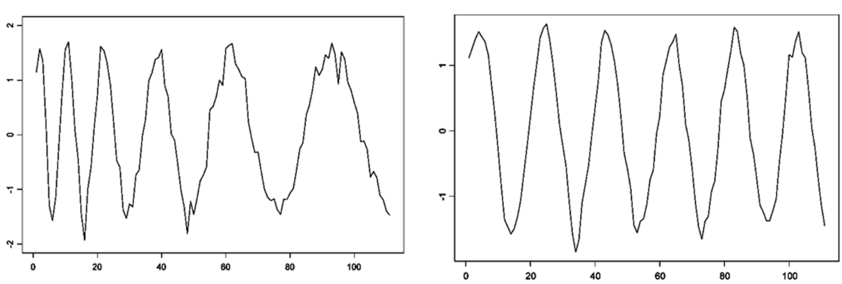

Figure 1. (a) A realization generated from (13); (b) the dual data associated with $\widehat{\Delta} = 18$ and $h = 1.01748$.

Table 1
Factor table for ARMA(2, 3) model for the dual data shown in Fig. 1(b)

	Absolute reciprocal of root	Frequency	M-frequency
AR factors			
$1 - 1.899B + .9992B^2$	0.9992	0.0504	2.9084
MA factors			
$1 - 1.692B + .799B^2$	0.8940	0.0524	3.0238
$1 + .416B$	0.4158	0.5000	28.8534

associated with the second-order MA factor is also very close to $f^* = 3$. This is consistent with the fact that an ARMA(2, 2) model with near canceling factors can be used as an approximate model for data of the form

$$X(t) = A\cos(2\pi f t + \psi) + n(t) \tag{14}$$

where $n(t)$ is random nose and ψ is uniform $[0, 2\pi]$. The residuals pass the Ljung and Box (1978) white noise test. The final fitted Euler(2, 3) model is:

$$(1 - 1.899B + 0.9992B^2)Z(h^k) = (1 - 1.692B + 0.799B^2)(1 + 0.416B)a(h^k). \tag{15}$$

In this example, the Euler(p, q) model is clearly more parsimonious than the Euler(p) fit. Also in Fig. 2(a) only a single sharp peak at about $f^* = 2.9$ appears in

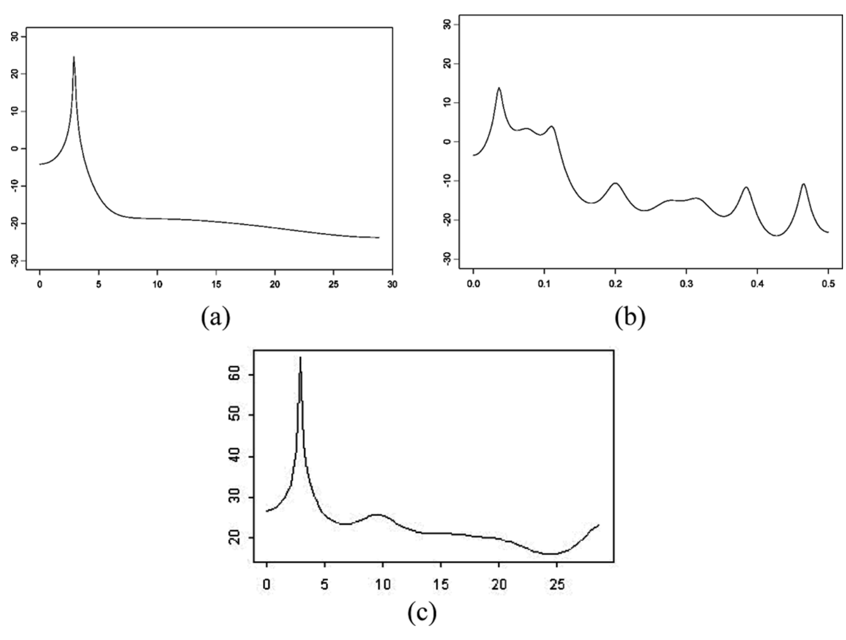

Figure 2. (a) M-spectrum based on the Euler(2, 3) model; (b) AR(10)-spectrum of the original data; (c) M-spectrum based on Euler(9) model.

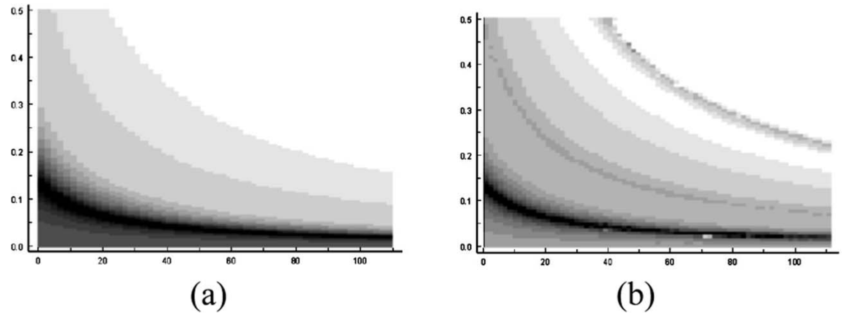

Figure 3. Instantaneous spectra (a) based on the Euler(2, 3) model and (b) based on the Euler(9) model.

the M-spectral density estimator based on the Euler(2, 3) model, while the energy is spread over a wide band from .03 to .14 in the AR(10) spectrum, shown in Fig. 2(b). This is typical of spectral estimation results obtained by fitting data of the form in (14) with an AR(p) model. In Fig. 2(c) we see that the M-spectrum for the Euler(9) fit has a single sharp peak but also has suggestions of other peaks at higher frequencies. In Figs. 3(a) and (b) we show the instantaneous spectra associated with the Euler(2, 3) and Euler(9) fits, respectively. In both cases it can be seen that the instantaneous frequency decreases from about $f = .14$ at the beginning of the series to less than $f = .05$ at the end. As with the M-spectrum, the instantaneous spectrum associated with the Euler(9) shows the effect of a non parsimonious model with associated spurious frequency behavior at higher instantaneous frequencies.

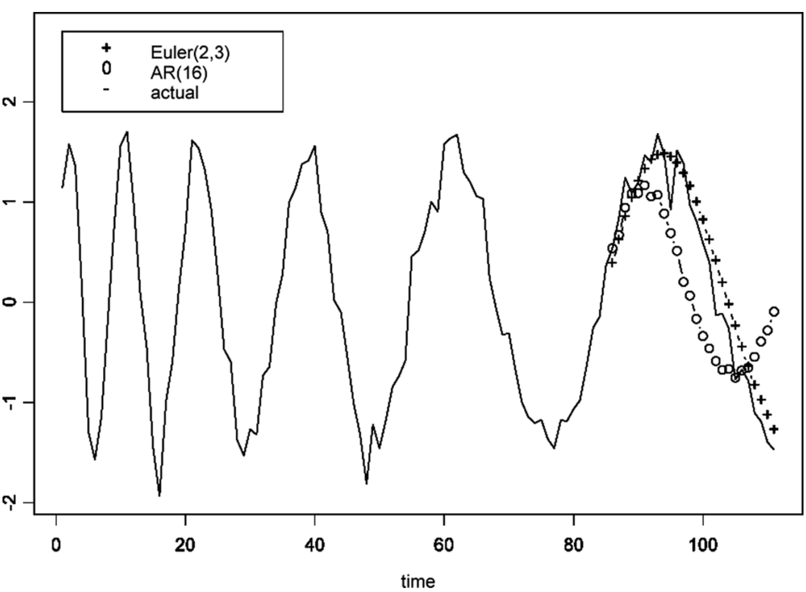

Figure 4. The plot of the last 25 steps of series forecast of Euler(2, 3) and AR(16) models, where (+++) and (o-o-o) indicate the forecasts based on the Euler(2, 3) and AR(16) fits, respectively.

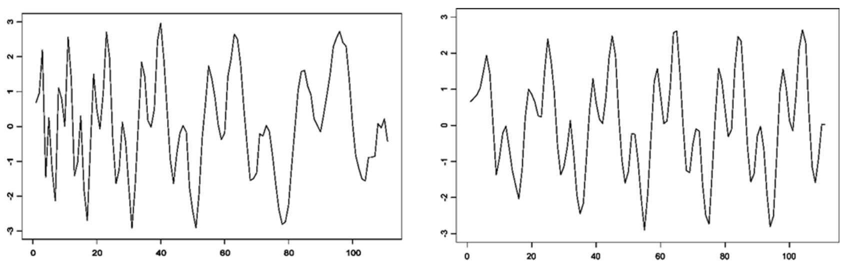

(a) (b)

Figure 5. (a) realization of length $n = 111$ from model (16) and (b) dual data associated with $h = 1.01791$ and origin offset 19.

Forecasts based on the Euler(2, 3) and AR(10) models are shown in Fig. 4. The forecasts of the last 25 points using the Euler(2, 3) model are very close to the actual data but the forecasts using the AR(10) are out of phase and die out more quickly in Fig. 4. More specifically, the mean square forecast errors (MSFE) for the last 25 time points of the series is 0.0148 for the Euler(2, 3) model and 0.8093 for the AR(10). Forecasts using the Euler(9) are similar to those obtained using the Euler(2, 3) model and are not shown here.

Example 3.2. Figure 5(a) shows a realization of length 111 from the series given by

$$X(t) = A\cos\left[2\pi f_1^* \ln(t+19) + v_1\right] + B\cos\left[2\pi f_2^* \ln(t+19) + v_2\right] + n(t), \tag{16}$$

which has sinusoidal behavior at M-frequencies, $f_1^* = 9$ and $f_2^* = 3$. The Euler(4, 4) model

$$\begin{aligned}(1 - 1.895B + .998B^2)&(1 - 1.146B + B^2)X(h^k)\\ &= (1 - 1.088B + .616B^2)(1 - 1.1742B + .349B^2)a(h^k)\end{aligned} \tag{17}$$

is fit to the data with $\widehat{\Delta} = 19$ and $h = 1.01791$. The factor table associated with the Euler(4, 4) is shown in Table 2. The estimated M-frequencies are 2.8899 and 8.6078 which are good estimates of the true M-frequencies, $f_1^* = 3$ and $f_2^* = 9$.

Table 2
Factor table associated with the Euler(4, 4), where $h = 1.01791$

	Absolute reciprocal of root	Frequency	M-frequency
AR factors			
$1 - 1.146B + .999B^2$	.9994	.1528	8.6078
$1 - 1.895B + .998B^2$	.9990	.0513	2.8899
MA factors			
$1 - 1.088B + .616B^2$	.7850	.1282	1.2510
$1 - 1.174B + .349B^2$	.5909	.0181	.1766

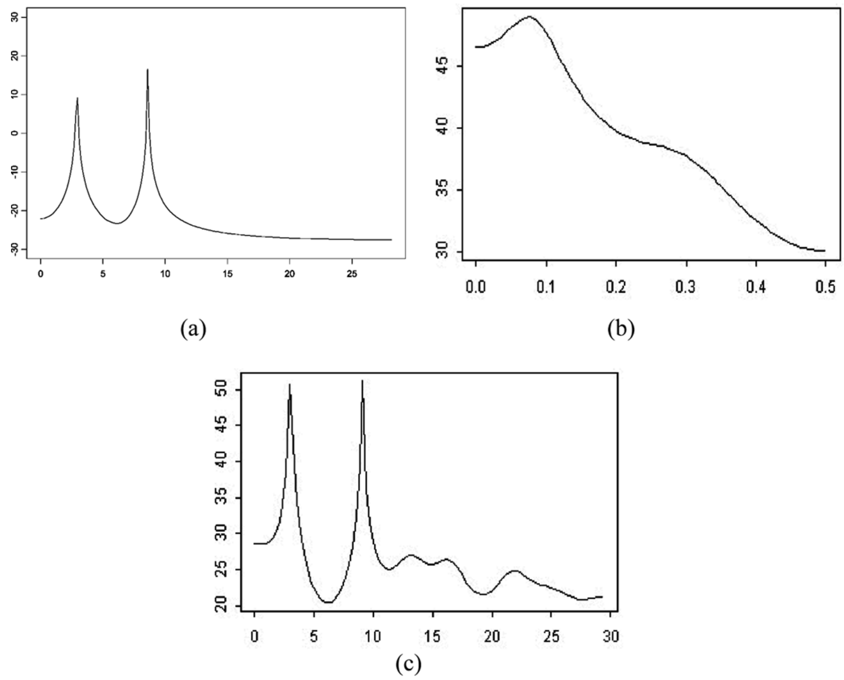

Figure 6. (a) M-spectral density estimator based on the Euler(4, 4) model; (b) AR(4)-spectral density; (c) M-spectral density based on Euler(14) model.

The dual process associated with the Euler(4, 4) fit is shown in Fig. 5(b), and it has the appearance of a process with two cycles that do not change with time. An AR(4) and an Euler(14) were selected as the best fitting AR and Euler(p) models fit to the original data. The M-spectrum based on the Euler(4, 4) fit is shown in Fig. 6(a) where two sharp peaks at about 2.9 and 8.6 appear. However, there is no prominent peak and the energy spreads over a wide range of frequencies in the AR(4) spectrum of the original process, shown in Fig. 6(b). The Euler(14) spectrum is shown in Fig. 6(c) where the two sharp peaks are apparent, but extraneous peaks appear at higher frequencies. The instantaneous spectra based on the Euler(4, 4)

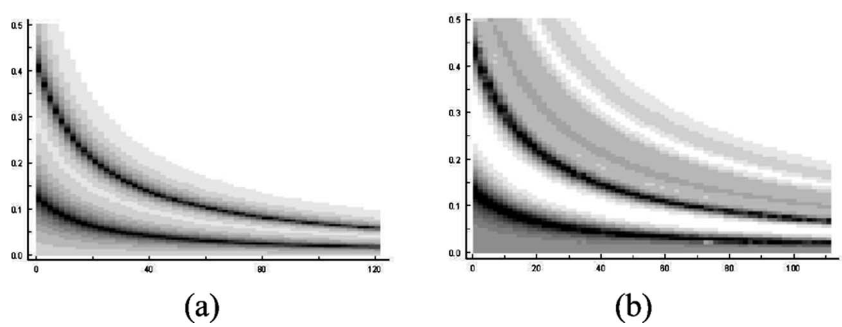

Figure 7. Instantaneous spectra based on (a) Euler(4, 4) and (b) Euler(14).

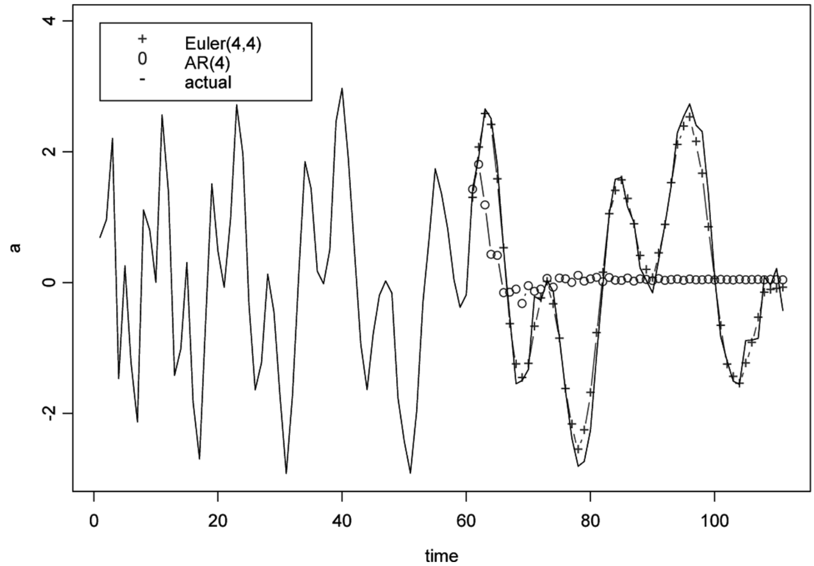

Figure 8. The plot of the last 40 steps of forecasts based on Euler(4, 4) and AR(4) models where (+++) and (o-o-o) indicate the forecasts based on the Euler(4, 4) and AR(4) fits, respectively.

and Euler(14) models are shown in Figs. 7(a) and (b), respectively, where the two instantaneous frequencies are clearly visible, but again the plot associated with the Euler(14) fit shows the effects of a non parsimonious fit.

The forecasts of the last 40 points based on the Euler(4, 4) and ARMA(6) models are shown in Fig. 8. There it can be seen that forecasts based on the Euler(4, 4) are very close to the actual data, while forecasts using the AR(4) model are out of phase and die out very fast. Again, the forecasts using the Euler(14) model are similar to those obtained using the Euler(4, 4) and are not shown here.

Example 3.3. A realization of length $n = 150$ generated from the Euler(2, 2) process

$$(1 - 1.7234B + .99B^2)X(h^k) = (1 - 1.37B + .72B^2)a(h^k), \tag{18}$$

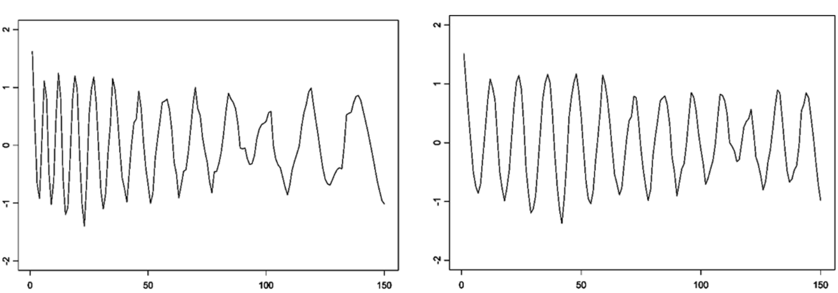

(a) (b)

Figure 9. (a) A realization from the Euler(2, 2) in (20); (b) the dual process associated with Euler(2, 3) fit.

Table 3
Factor tables associated with Euler(2, 3) models

	Absolute reciprocal of root	Frequency	M-frequency
AR factors			
$1 - 1.7195B + .9011B^2$	.9955	.0841	8.4027
MA factors			
$1 - 1.368B + .718B^2$	.8471	.1004	10.0312
$1 + .559B$	.5594	.5000	49.9563

is shown in Fig. 9(a) where $\sigma_a^2 = 0.03$ and $\Delta = 40$. It can be seen that the data have a cyclical behavior with periods that elongate. For this realization, an Euler(2, 3) model with $h = 1.010059$ and $\widehat{\Delta} = 42$ is fit to the data. The fitted model is given by

$$(1 - 1.7195B + .9911B^2)X(h^k) = (1 - .8088B - .0477B^2 + .4014B^3)a(h^k), \qquad (19)$$

and diagnostic tests indicate a suitable fit. The coefficients and system frequencies of the Euler(2, 3) model, shown in Table 3, are close to those of the Euler(2, 2) in

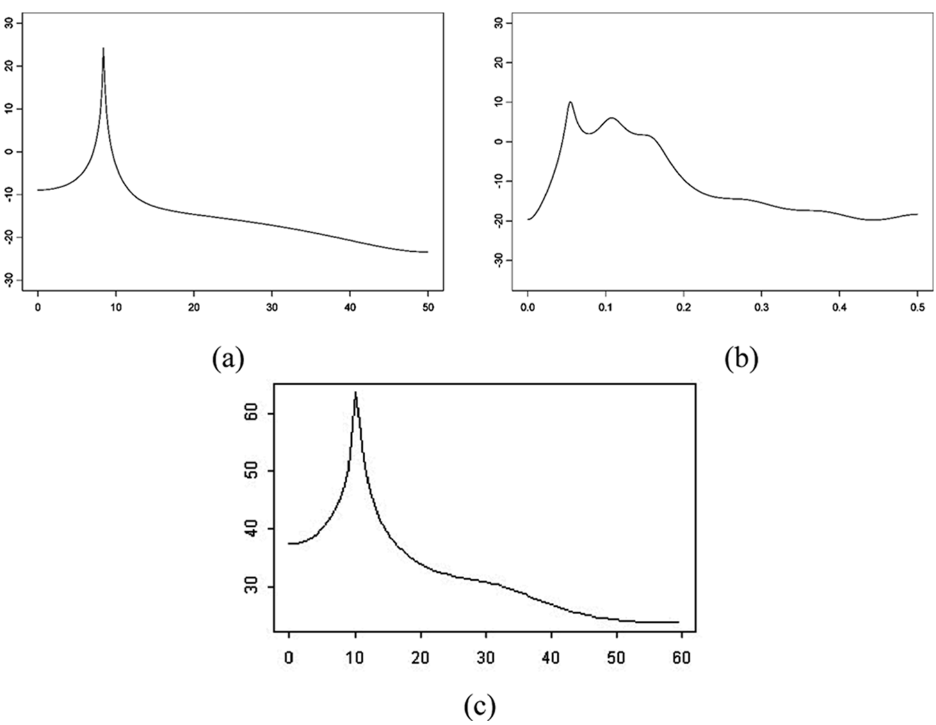

Figure 10. Spectral plots associated with the Euler(2, 2) data in Fig. 9(a): (a) M-spectral density based on the Euler(2, 3) model; (b) spectral density estimator based on the ARMA(11, 1) model; (c) M-spectral density based on Euler(5) fit.

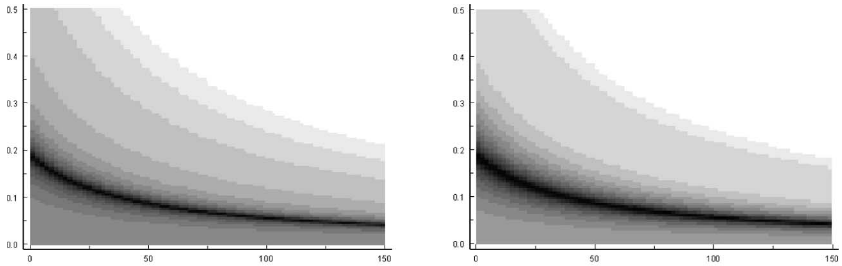

(a) (b)

Figure 11. Instantaneous spectra for the Euler(2, 2) data in Fig. 9(a): (a) based on Euler(2, 3); (b) based on Euler(5) fit.

(18) from which the data were generated. An Euler(5) model is fit to the data when the dual model is restricted to be an AR(p). Using standard procedures for fitting an ARMA(p, q) model to the original data, an ARMA(11, 1) model was selected.

The dual process associated with the Euler(2, 3) fit is shown in Fig. 9(b) where there are approximately 12 points in each dual cycle which is consistent with the single peak at $f^* = 8.4$ in the M-spectrum based of the Euler(2, 3) shown in Fig. 10(a). The spectrum based on the ARMA(11, 1) fit is shown in Fig. 10(b) and it does not show a distinct peak and indicates periodic behavior over a wide range of frequencies from 0 to .2. In Fig. 10(c) the M-spectrum associated with the Euler(5) model fit to the data shows a single dominant peak at about $f^* = 10$ and a very small spurious peak at about $f^* = 30$. In Figs. 11(a) and (b) are shown the instantaneous spectra for the Euler(2, 3) and Euler(5) fits, respectively. These instantaneous spectra are quite similar.

4. Application of Euler(p, q) Processes to Real Data

Bat echolocation calls are known to contain frequencies that vary over time. In this section, we will apply Euler(p, q) processes to a signal of length $n = 96$ from

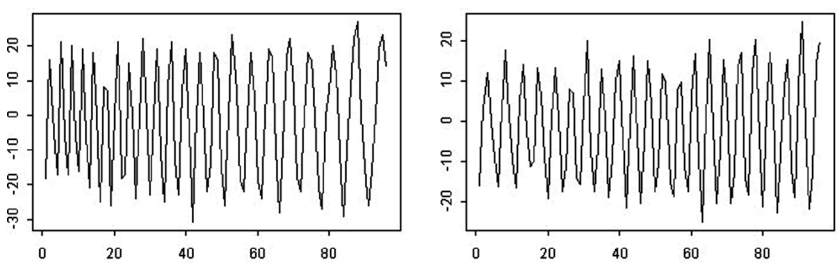

(a) (b)

Figure 12. (a) The plot of Noctule bat signal of size 96; (b) The dual process of the Noctule bat signal based on an Euler(2, 2) model.

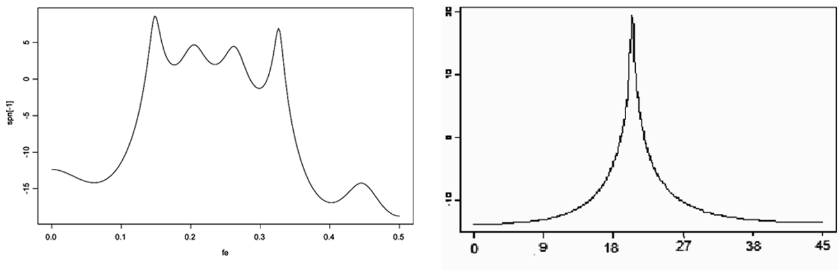

(a) (b)

Figure 13. (a) The AR(12)-spectrum of the original Noctule bat signal; (b) The M-spectrum based on the Euler(2, 2) with $h = 1.01121$ and origin offset 49.

a *Nyctalus noctula* (Noctule) bat. The bat calls are taken at 25 kHz, and the data are shown in Fig. 12(a). Using standard procedures, an AR(12) model is fit to the original data, and the corresponding AR(12) spectral estimate is shown in Fig. 13(a) where it can be seen that the spectrum is spread over several frequencies none of which are dominant. This type of spectrum is typical of data with time-varying frequencies as we have seen in the case of the simulated realizations in the previous examples. Using the procedure described in this article we fit an Euler(2, 2) model with $\widehat{\Delta} = 49$ and $h = 1.01121$. A dominant cycle of about 5 time units is seen in the dual process, shown in Fig. 12(b). The factor table is shown in Table 4. As we expect from the dual process, there is a sharp peak at around 20.46 in the M-spectrum based on the Euler(2, 2) model.

The instantaneous spectrum associated with the Euler(2, 2) fit is shown in Fig. 14(a) where it can be seen that the instantaneous frequency decreases from about $f = .4$ at the beginning of the signal to about $f = .15$ at the end. In Fig. 14(b) we show the Wigner–Ville spectrum (see Mecklenbräuker and Hlawatsch, 1997) which gives similar results except for the fact that the estimates break down at the beginning and end of the series as is typical of such window-based methods. The results given here indicate that a logarithmic transformation of time is appropriate for stationarizing the bat signal.

Table 4
Factor tables associated with Euler(2, 2) models for the *Noctule* bat data

	Absolute reciprocal of root	Frequency	M-frequency
AR factors			
$1 - .272B + .983B^2$	.9916	.2281	20.46
MA factors			
$1 - .163B + .252B^2$	.5022	.2241	20.10

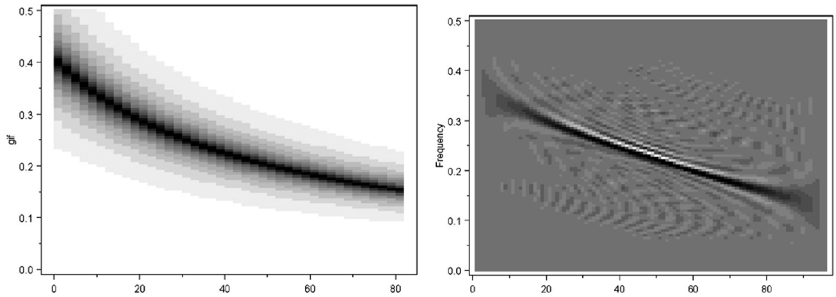

(a) (b)

Figure 14. (a) Instantaneous spectrum for Noctule bat signal in Figs. 12(a) and (b) the Wigner–Ville plot.

5. Concluding Remarks

In this article we have defined continuous and discrete Euler(p, q) processes and developed their properties. It is shown that sampling a continuous Euler(p, q) process at Euler time points, h^k for $h > 1$ and $k = 0, 1, \ldots, n$, leads to a realization from a discrete Euler(p, r) process where $r \leq p - 1$. We show that the Euler(p, q) can be used to find parsimonious models in much the same sense that the ARMA model can provide more parsimonious representations than an AR model in many cases. In addition, we point out that Jiang et al. (2006) describe time deformation based on the Box-Cox transformation that includes the logarithmic transformation considered here as a special case. It is also possible to consider ARMA as well as AR models for the resulting dual processes in that setting.

References

Akaike, H. (1973). Information theory and an extension of the maximum likelihood principle. In: Petrov, B. N., Csaki, F., eds. *2nd Int. Symp. Inform. Theor*. Budapest: Akademiai Kiado, pp. 267–281.

Akaike, H. (1974). A new look at statistical model identification. *IEEE Trans. Automatic Control* AC-19:716–723.

Choi, E.-H. (2003). EARMA Processes with Spectral Analysis of Nonstationary Time Series. Ph.D. Dissertation, Department of Statistical Science, Southern Methodist University, Dallas, TX, USA.

Gray, H. L., Zhang, N. (1988). On a class of nonstationary processes. *J. Time Ser. Anal.* 9:133–154.

Gray, H. L., Vijverberg, C. P., Woodward, W. A. (2005). Nonstationary data analysis by time deformation. *Commun. Statist. A* 34:163–192.

Jiang, H., Gray, H. L., Woodward, W. A. (2006). Time-frequency analysis: $G(\lambda)$ processes. *Computat. Statist. Data Anal.* Vol. 51. doi: 10.1016/j.csda.2005.12.011, to be published.

Ljung, G. M., Box, G. E. P. (1978). On a measure of a lack of fit in time series models. *Biometrika* 65:297–303.

Mecklenbräuker, W., Hlawatsch, F., eds. (1997). *The Wigner Distribution—Theory and Applications in Signal Processing*. Amsterdam: Elsevier.

Phadke, M. S., Wu, S. M. (1974). Modeling of continuous stochastic processes from discrete observations with application to sunspots data. *J. Amer. Statist. Assoc.* 69:325–329.

Priestley, M. B. (1981). *Spectral Analysis and Time Series: Volume 1 – Univariate Series*. London: Academic Press.

Vijverberg, C. P. (2002). Discrete Multiplicative Stationary Processes. Ph.D. Dissertation, Department of Statistical Science, Southern Methodist University, Dallas, TX, USA.

Woodward, W. A., Gray, H. L. (1983). A comparison of autoregressive and harmonic component models for the lynx data. *J. Roy. Statist. Soc.* A146:71–73.